Acta Crystallographica Section C
**Crystal Structure Communications**
ISSN 0108-2701

# New organic–inorganic frameworks incorporating iso- and heteropolymolybdate units and a 3,3′,5,5′-tetramethyl-4,4′-bi-1*H*-pyrazole-2,2′-diium multiple hydrogen-bond donor

**Liliana V. Lukashuk,[a] Andrey B. Lysenko,[a] Harald Krautscheid[b] and Konstantin V. Domasevitch[a]***

[a]Inorganic Chemistry Department, National Taras Shevchenko University of Kyiv, Volodimirska Street 64, Kyiv 01033, Ukraine, and [b]Institute of Inorganic Chemistry, Leipzig University, Johannisallee 29, D-04103 Leipzig, Germany
Correspondence e-mail: dk@univ.kiev.ua

Received 29 July 2011
Accepted 8 November 2011
Online 16 November 2011

Poly[bis(3,3′,5,5′-tetramethyl-4,4′-bi-1*H*-pyrazole-2,2′-diium) $\gamma$-octamolybdate(VI) dihydrate], $\{(C_{10}H_{16}N_4)_2[Mo_8O_{26}]\cdot 2H_2O\}_n$, (I), and bis(3,3′,5,5′-tetramethyl-4,4′-bi-1*H*-pyrazole-2,2′-diium) $\alpha$-dodecamolybdo(VI)silicate tetrahydrate, $(C_{10}H_{16}N_4)_2[SiMo_{12}O_{40}]\cdot 4H_2O$, (II), display intense hydrogen bonding between the cationic pyrazolium species and the metal oxide anions. In (I), the asymmetric unit contains half a centrosymmetric $\gamma$-type $[Mo_8O_{26}]^{4-}$ anion, which produces a one-dimensional polymeric chain by corner-sharing, one cation and one water molecule. Three-centre bonding with 3,3′,5,5′-tetramethyl-4,4′-bi-1*H*-pyrazole-2,2′-diium, denoted $[H_2Me_4bpz]^{2+}$ [N$\cdots$O = 2.770 (4)–3.146 (4) Å], generates two-dimensional layers that are further linked by hydrogen bonds involving water molecules [O$\cdots$O = 2.902 (4) and 3.010 (4) Å]. In (II), each of the four independent $[H_2Me_4bpz]^{2+}$ cations lies across a twofold axis. They link layers of $[SiMo_{12}O_{40}]^{4-}$ anions into a three-dimensional framework, and the preferred sites for pyrazolium/anion hydrogen bonding are the terminal oxide atoms [N$\cdots$O = 2.866 (6)–2.999 (6) Å], while anion/aqua interactions occur preferentially *via* $\mu_2$-O sites [O$\cdots$O = 2.910 (6)–3.151 (6) Å].

## Comment

Pyrazole species attract general interest as versatile multipurpose tectons for the development of solid-state architecture (Halcrow, 2009). In this respect, bifunctional 3,3′,5,5′-tetramethyl-4,4′-bipyrazole ($Me_4bpz$) offers special potential as a symmetric neutral or anionic linker for discrete polynuclear complexes (Yu *et al.*, 2005), open metal–organic polymers for adsorption applications (Zhang & Kitagawa, 2008; Rusanov *et al.*, 2003), acentric hydrogen-bonded frameworks (Boldog *et al.*, 2001) and binary cocrystals (Boldog *et al.*, 2004). Even wider applications for the development of hydrogen-bonded structures could be anticipated for the 3,3′,5,5′-tetramethyl-4,4′-bi-1*H*-pyrazole-2,2′-diium dication, $[H_2Me_4bpz]^{2+}$. The cation may be viewed as a symmetric donor of four hydrogen bonds, while a particular benefit of the tecton structure arises from the spatial proximity of two NH groups supported by each of the pyrazolium rings. The latter favours multiple and multicentre interactions with the anionic substrate, which could be especially relevant for polynuclear and polymeric oxo- and halometallate anions, providing a number of closely separated hydrogen-bond acceptor sites. Therefore, bipyrazolium tectons may be applied as very specific cationic templates for metal–oxide materials, such as layered molybdenum(VI) and vanadium(V) oxides and low-dimensional isopolymolybdates(VI) (Hubbard *et al.*, 2008; Hagrman *et al.*, 1999). In this context, we have prepared two new salts, poly[bis(3,3′,5,5′-tetramethyl-4,4′-bi-1*H*-pyrazole-2,2′-diium) $\gamma$-octamolybdate(VI) dihydrate], (I), and bis(3,3′,5,5′-tetramethyl-4,4′-bi-1*H*-pyrazole-2,2′-diium) $\alpha$-dodecamolybdo(VI)silicate tetrahydrate, (II), based on the $[H_2Me_4bpz]^{2+}$ cation and iso- and heteropolymolybdate anionic species, and report their structures here. Only a few previous works have considered the special supramolecular significance of hydrogen-bonded pyrazolium cations (Boldog *et al.*, 2009; Singh *et al.*, 2011).

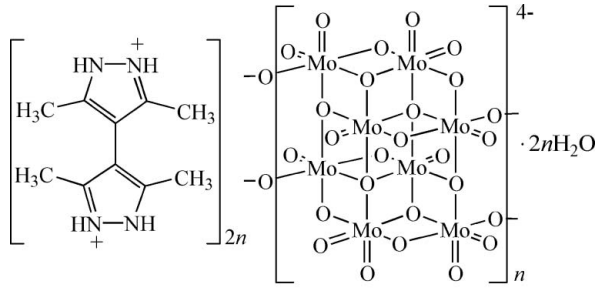

(I)

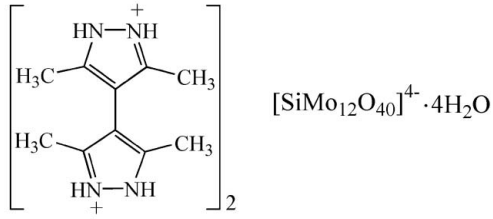

(II)

The structure of (I) consists of one-dimensional polymolybdate anions running along the crystallographic *a* direction, $[H_2Me_4bpz]^{2+}$ dications and solvent water molecules. The inorganic polyanion is built up of repeating centrosymmetric $[Mo_8O_{26}]^{4-}$ units sharing two pairs of opposite vertices and the corresponding oxide bridge is actually linear: Mo4—O12—Mo2$^{ii}$ = 174.18 (14)° [symmetry code: (ii) $-x$, $-y+1$, $-z+1$] (Fig. 1). The molecular shape and functionality of the $[H_2Me_4bpz]^{2+}$ template is important for the structure of the infinite metal–oxide anion. The present connection mode is characteristic of polymeric octamolybdates crystallized as salts of the organic bases 4-aminopyridine (Nelson *et al.*, 2006),

  doi:10.1107/S0108270111047159 

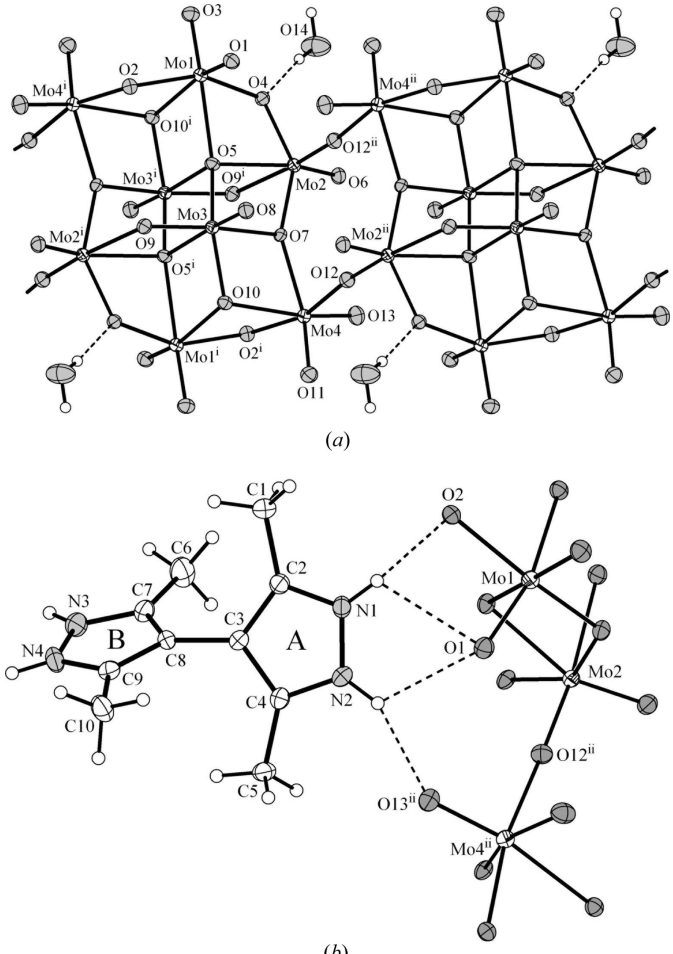


**Figure 1**
(*a*) The inorganic anion in the environment of the solvent water molecules and (*b*) the organic dication in the structure of (I), showing the atom-labelling scheme. Displacement ellipsoids are drawn at the 40% probability level. The dashed lines indicate hydrogen bonding. [Symmetry codes: (i) $-x+1, -y+1, -z+1$; (ii) $-x, -y+1, -z+1$.]

*N*,*N*-dimethylethylenediamine (Thorn *et al.*, 2005) and 1,4-diazabicyclo[2.2.2]octane (Fang *et al.*, 2004), while the long cationic templates hexane-1,6-diamine (Xu *et al.*, 1996) and 1,1′-[(biphenyl-4,4′-diyl)dimethylene]diimidazole (Liu *et al.*, 2010) produce an isomeric one-dimensional polyoctamolybdate array. The $[Mo_8O_{26}]^{4-}$ units themselves adopt the $\gamma$-isomeric form of octamolybdate (Hagrman *et al.*, 1999), with the typical octahedral environment of each metal ion involving three types of Mo—O bonds (2+2+2 coordination), *viz.* short molybdenyl bonds with terminal oxide ligands [1.693 (2)–1.717 (2) Å], Mo—$\mu_2$-O [1.901 (2)–1.977 (2) Å] and longer Mo—O bonds [2.173 (2)–2.438 (2) Å], with four $\mu_3$-oxide and two $\mu_4$-oxide ligands.

Interaction of the bipyrazolium dications and one-dimensional oxoanions occurs by means of extensive N—H···O hydrogen bonding, utilizing most of the terminal O atoms (O1, O6, O8 and O13), as well as the $\mu$-oxide O2 and O10 centres (Table 1). This is responsible for the connection of the components into hydrogen-bonded layers parallel to the *ac* plane (Fig. 2). Within these layers, successive oxide chains are situated at a distance of 12.9231 (13) Å (parameter *c* of the unit cell). Each pyrazolium ring is involved in bonding with two adjacent $[Mo_8O_{26}]^{4-}$ units along the chain. The high number of closely situated O-atom acceptor sites effects bifurcation of the hydrogen-bond interactions. This is a salient feature of such a system and it could be considered as a design tool. In this way, pyrazole ring *A* (N1/N2/C2–C4; Fig. 1*b*) adopts four hydrogen bonds with three acceptor atoms (N—H···O = 112–152°), which is important for the densest accommodation of the cation on the metal oxide matrix (Fig. 2). The bonding mode of ring *B* (N3/N4/C7–C9; Fig. 1*b*) is slightly different, with one three-centre bond of the N3—H donor and one directional N4—H4···O10($-x+1, -y+1, -z+2$) interaction with a single acceptor site, which provides the shortest N···O contact [2.724 (4) Å]. Other N···O separations [2.770 (4)–3.146 (4) Å] (Table 1) are also typical for N—H···O hydrogen bonds. However, they are slightly longer than the parameters derived from a statistical evaluation of pyrazolium salts (2.62–2.94 Å, distribution median = 2.74 Å; Boldog *et al.*, 2009) due to bifurcation of the bonds. The present three-centre hydrogen bonding may be especially relevant for pyrazolium salts involving a high number of convenient acceptors, as provided by polyoxometallate species. This situation may also be related to the hydrogen-bonding patterns of 4,4′-bipyrazolium fluorometallate salts based on $[TaF_6]^-$, $[Zr_2F_{12}]^{4-}$ and $[BeF_3^-]_n$ anions (Boldog *et al.*, 2009). Hydrogen bonds with water molecules extends this structure in the third dimension, with the formation of centrosymmetric anion–aqua fragments $MoO_6$–$(HOH)_2$–$O_6Mo$ involving two terminal and two $\mu_2$-O-atom acceptors (Fig. 2*b*). The O···O separations in the latter cases are slightly shorter, *viz.* 2.902 (4) *versus* 3.010 (4) Å for O···O(terminal) (Table 1).

The asymmetric unit of (II) includes an $[SiMo_{12}O_{40}]^{4-}$ anion, four half $[H_2Me_4bpz]^{2+}$ dications and four water molecules (Fig. 3). The complete organic molecules are generated by crystallographic twofold symmetry. The $[SiMo_{12}O_{40}]^{4-}$ anions adopt the most common $\alpha$-form, with the typical distorted octahedral coordination of 12 Mo atoms, which involve short bonds with terminal oxide ligands [Mo—O = 1.684 (4)–1.711 (4) Å] and elongated bonds with a $\mu_4$-O atom in a *trans* position [Mo—O = 2.315 (3)–2.385 (5) Å]. Four equatorial Mo—O bonds with $\mu_2$-O ligands are in the range 1.824 (3)–2.043 (4) Å.

The anions, water molecules and 3,5-dimethylpyrazolium halves of the $[H_2Me_4bpz]^{2+}$ tectons form clearly distinguishable hydrogen-bonded layers parallel to the *bc* plane (interlayer separation = 0.5*a* = 11.27 Å) (Fig. 4). This array is dominated by the packing of the very bulky anions and thus the pyrazolium and water hydrogen-bond donors appear intercalated in the voids of these layers. Hydrogen bonding between the $[H_2Me_4bpz]^{2+}$ and $[SiMo_{12}O_{40}]^{4-}$ counterparts is itself weaker and less characteristic than in the case of (I). Firstly, for all four independent cations, only half of the NH donors interact directly with the metal oxide matrix, while the other interactions are expanded by inclusion of a water molecule: NH···OH···OMo (Fig. 4). This parallels the binding mode of $[H_2Me_4bpz]^{2+}$ and the much smaller low nucleophilic

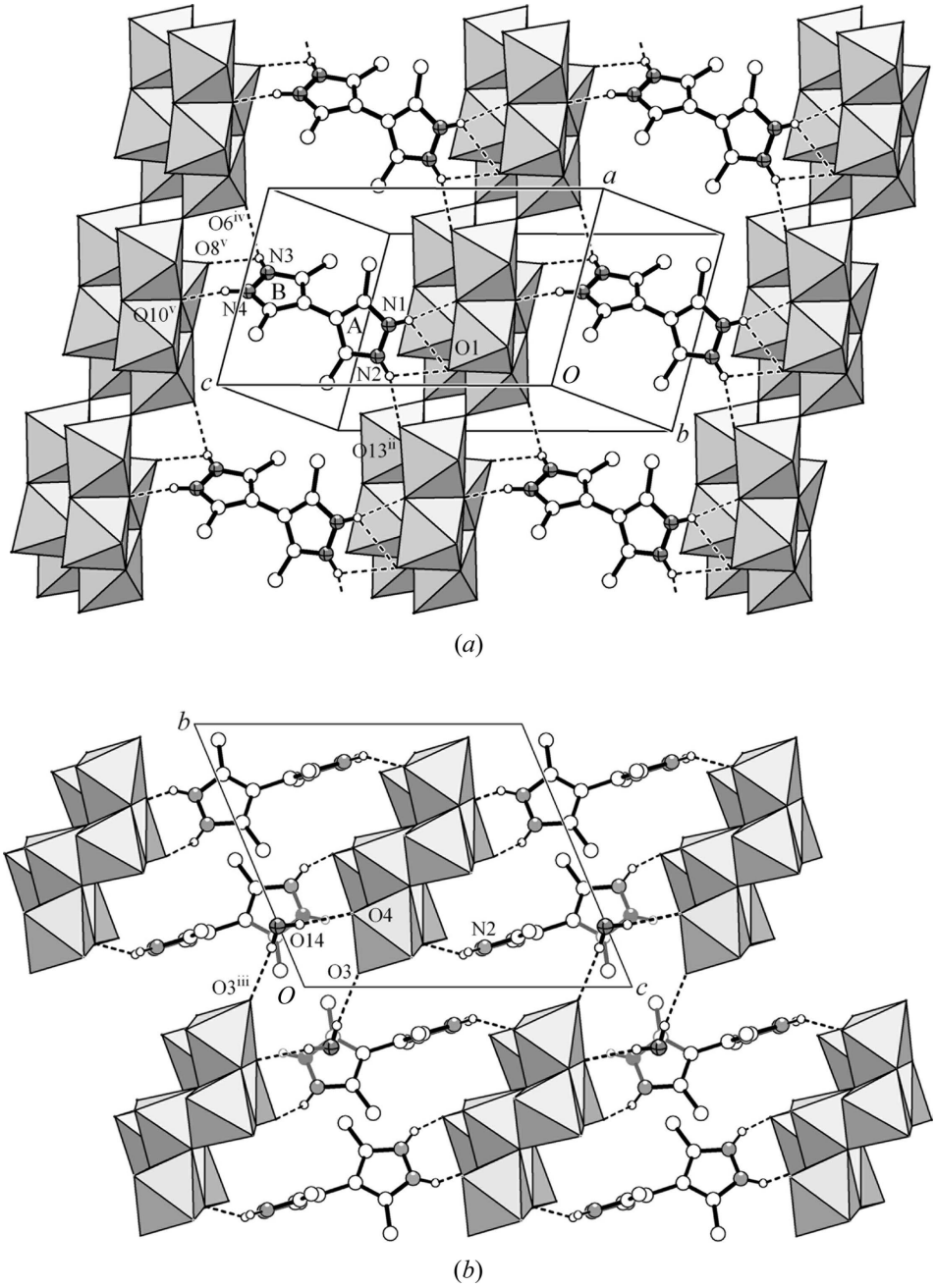


**Figure 2**
(*a*) The hydrogen-bonded layer in the structure of (I), showing a set of three-centre interactions between the one-dimensional oxometallate chains (in a polyhedral representation) and bipyrazolium connectors. (*b*) A projection onto the *bc* plane, showing the mode of connection of the $\{(H_2Me_4bpz)_2[Mo_8O_{26}]\}_n$ layers by water molecules. Note the centrosymmetric aqua–molybdate motif. C-bound H atoms have been omitted for clarity. [Symmetry codes: (ii) $-x, -y+1, -z+1$; (iii) $-x, -y, -z$; (iv) $x+1, y, z+1$; (v) $-x+1, -y+1, -z+2$.]

anion $S_2O_6^{2-}$ (Boldog *et al.*, 2009). Secondly, the present N—H···O(Mo) hydrogen bonds [2.866 (6)–3.285 (6) Å] are appreciably longer than the N—H···$OH_2$ hydrogen bonds [2.693 (6)–2.864 (7) Å] (Table 3) and also longer than the N—H···O(Mo) hydrogen bonds in the case of (I). This reflects the weakness of the hydrogen bonding and such an observation may be related to only a very weak hydrogen-bond interaction in the $(PyH)_4[SiMo_{12}O_{40}]\cdot 0.5H_2O$ salt [N···O = 3.05 (1)–3.29 (1) Å; PyH is pyridinium] (Dang & Jin, 2007).

Similar to (I), the preferred anion sites for establishing hydrogen bonds with the pyrazolium cation are the terminal oxide ligands (Fig. 3). For (II), weak interactions with $\mu_2$-O atoms [N···O = 3.041 (6) and 3.285 (6) Å] exist only as longer branches of three-centre bonds (Table 3). The present discrimination of the acceptor sites is likely predetermined by the relative negative charge located at the O atoms. Thus, the bond-valence sum calculations for (I) and (II) (Tables 2 and 4) suggest that the terminal oxide ligands are the most underbonded and highly nucleophilic (Tytko *et al.*, 1999). The same situation is reflected in the N—H···O hydrogen bonding with the $\mu_2$-O and $\mu_3$-O acceptors in (I), which occurs *via* the most nucleophilic sites O2 and O10 (Table 2). Steric accessibility of

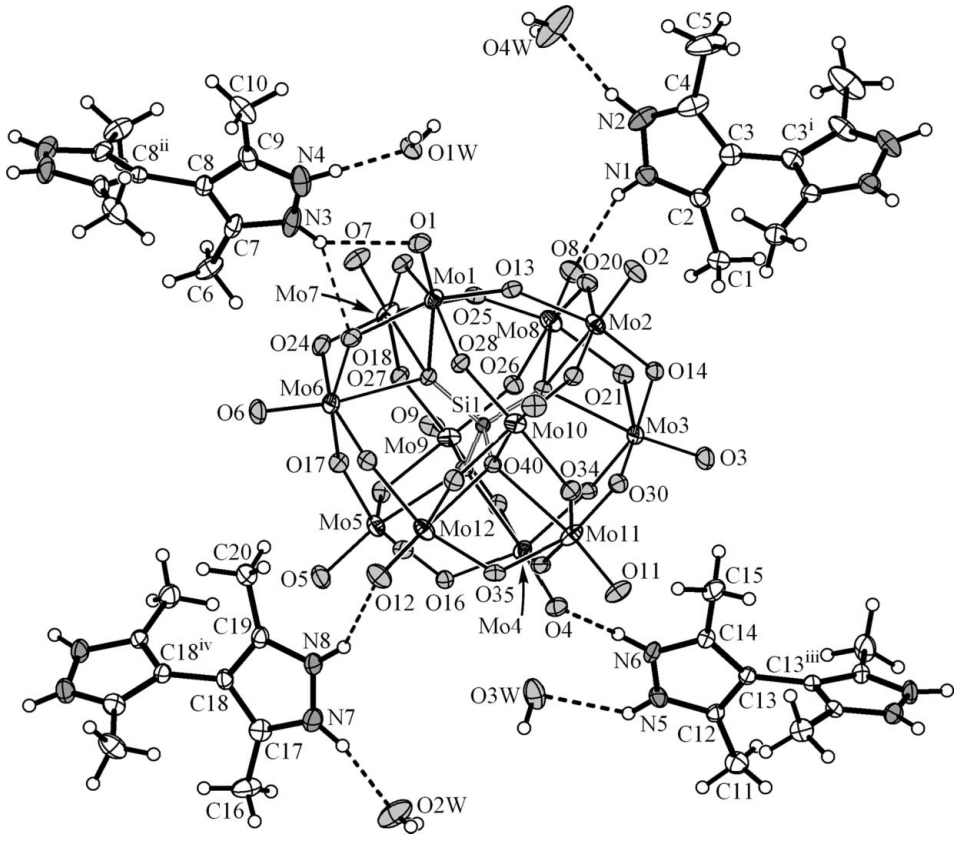


**Figure 3**
The structure of (II), showing the atom-labelling scheme. Displacement ellipsoids are drawn at the 40% probability level. N and O atoms are shaded grey and dashed lines indicate hydrogen bonding. [Symmetry codes: (i) $-x, y, -z+1$; (ii) $-x+1, y, -z+3$; (iii) $-x, y, -z$; (iv) $-x+1, y, -z+2$.]

the terminal O atoms is the second important factor when considering the bulk volume of the dimethylpyrazolium substrate. It is notable that the hydrogen bonding of small water molecules in (II) occurs preferentially with $\mu_2$-O atoms (Table 4).

In both structures, the organic tectons exhibit a typical twisted conformation [for (I), the C2—C3—C8—C7 torsion angle is 62.7 (5)°; for (II), the corresponding angles are in the range 64.1 (8)–75.0 (8)°]. The equivalence of the pyrazolium NH sites is best indicated by the angles at the N atoms (Domasevitch, 2008). They are actually uniform in all cases [108.9 (3) and 109.0 (3)° in (I), and in the range 108.6 (5)–110.7 (5)° in (II)], while a neutral $Me_4$bpz molecule ($\alpha$-polymorph) displays a differentiation of these parameters according to the types C—N—N(H) = 104.1 (2)° and C—N(H)—N = 113.0 (2)° (Boldog *et al.*, 2001).

In brief, the specific hydrogen-bond donor fuctionality of the pyrazolium group is well suited to the formation of multiple interactions with the polyoxometallate matrix, and bifunctional pyrazoles may be viewed as a new type of organic template for the synthesis of molybdate materials.

## Experimental

The title compounds were synthesized by a hydrothermal technique starting with 3,3′,5,5′-tetramethyl-4,4′-bipyrazole ($Me_4$bpz; Boldog *et al.*, 2001). Compound (I) was obtained in the presence of cadmium(II) ions. For the preparation of (I), $Me_4$bpz (9.5 mg, 0.05 mmol), $(NH_4)_6Mo_7O_{24}\cdot 4H_2O$ (37.1 mg, 0.03 mmol), $CdCl_2\cdot 2.5H_2O$ (6.0 mg, 0.026 mmol) and water (4 ml) were placed in a Teflon vessel which was in turn placed in a steel bomb and heated at 443 K for 48 h. Cooling of the mixture to room temperature over a period of 72 h yielded colourless prisms of $(H_2Me_4bpz)_2[Mo_8O_{26}]\cdot 2H_2O$, (I) (yield 32 mg, 80%, based on the pyrazole base). For the preparation of (II), $Me_4$bpz (9.5 mg, 0.05 mmol), $H_4[SiMo_{12}O_{40}]\cdot 13H_2O$ (61.7 mg, 0.03 mmol) and water (5 ml) were sealed in a Pyrex tube, heated at 423 K for 24 h and then cooled to room temperature over a period of 48 h. Large yellow crystals of (II) were obtained in a yield of 38 mg (65%).

### Compound (I)

*Crystal data*

$(C_{10}H_{16}N_4)_2[Mo_8O_{26}]\cdot 2H_2O$
$M_r$ = 1604.09
Triclinic, $P\overline{1}$
$a$ = 8.0821 (8) Å
$b$ = 11.2521 (11) Å
$c$ = 12.9231 (13) Å
$\alpha$ = 106.242 (8)°
$\beta$ = 106.063 (9)°
$\gamma$ = 106.102 (8)°
$V$ = 1000.9 (2) Å$^3$
$Z$ = 1
Mo $K\alpha$ radiation
$\mu$ = 2.53 mm$^{-1}$
$T$ = 173 K
0.14 × 0.12 × 0.08 mm

*Data collection*

Stoe IPDS diffractometer
Absorption correction: numerical [*X-RED* (Stoe & Cie, 2001) and *X-SHAPE* (Stoe & Cie, 1999)]
$T_{min}$ = 0.718, $T_{max}$ = 0.823
9228 measured reflections
4505 independent reflections
3837 reflections with $I > 2\sigma(I)$
$R_{int}$ = 0.032

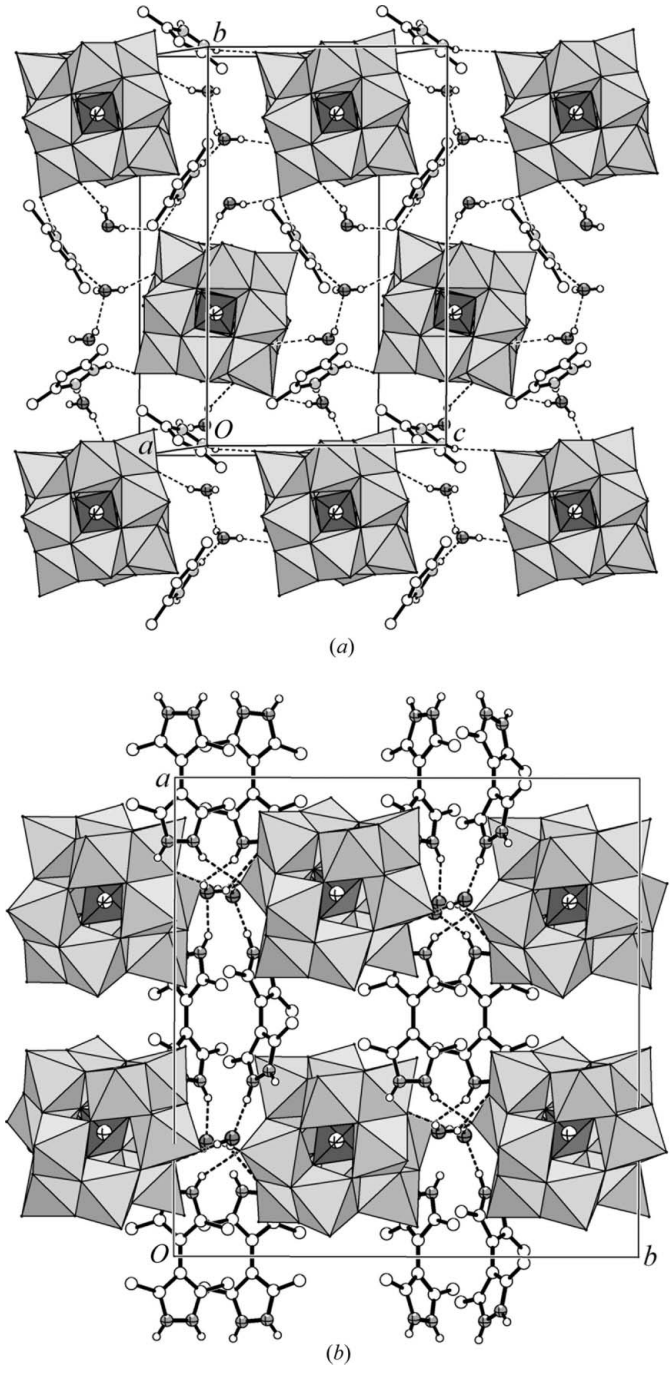


**Figure 4**
(*a*) The hydrogen-bonded layer in the structure of (II), showing how the pyrazolium and aqua hydrogen-bond donors are situated between the bulky $[SiMo_{12}O_{40}]^{4-}$ anions (depicted in a polyhedral representation). (*b*) A projection onto the *ab* plane, showing the $[H_2Me_4bpz]^{2+}$ tectons as links between successive hydrogen-bonded layers. N and O atoms are shaded grey and dashed lines indicate hydrogen bonding. C-bound H atoms have been omitted for clarity.

*Refinement*

$R[F^2 > 2\sigma(F^2)] = 0.024$
$wR(F^2) = 0.060$
$S = 0.98$
4505 reflections
293 parameters
H-atom parameters constrained
$\Delta\rho_{max} = 0.74$ e Å$^{-3}$
$\Delta\rho_{min} = -0.74$ e Å$^{-3}$

**Table 1**
Hydrogen-bond geometry (Å, °) for (I).

| $D$—H···$A$ | $D$—H | H···$A$ | $D$···$A$ | $D$—H···$A$ |
|---|---|---|---|---|
| O14—H1$W$···O3$^{iii}$ | 0.85 | 2.16 | 3.010 (4) | 173 |
| O14—H2$W$···O4 | 0.85 | 2.06 | 2.902 (4) | 173 |
| N1—H1···O2 | 0.88 | 1.96 | 2.770 (4) | 152 |
| N1—H1···O1 | 0.88 | 2.44 | 2.882 (4) | 112 |
| N2—H2···O13$^{ii}$ | 0.88 | 2.18 | 2.940 (4) | 144 |
| N2—H2···O1 | 0.88 | 2.33 | 2.830 (4) | 116 |
| N3—H3···O6$^{iv}$ | 0.88 | 2.13 | 2.838 (4) | 137 |
| N3—H3···O8$^{v}$ | 0.88 | 2.48 | 3.146 (4) | 133 |
| N4—H4···O10$^{v}$ | 0.88 | 1.95 | 2.724 (4) | 147 |

Symmetry codes: (ii) $-x, -y+1, -z+1$; (iii) $-x, -y, -z$; (iv) $x+1, y, z+1$; (v) $-x+1, -y+1, -z+2$.

**Table 2**
Bond-valence sums for $[Mo_8O_{26}]^{4-}$ and hydrogen-bond functionality of the oxide ligands in (I).

The valence sums are calculated with the formula $S_i = \exp[(R_0 - R_i)/B]$, where $S_i$ is the bond valence of bond $i$, $R_0$ is a constant dependant on the bonded elements [$R_0$(Mo—O) = 1.907], $R_i$ is the bond length of bond $i$ and $B = 0.370$. $\Sigma S_i$ is the bond-valence sum for the O atom and $V$ is the predicted valence for a site. The bond-valence sums for the Mo atoms are $\Sigma S_i = 5.871$–$5.940$.

| O atom | Type | Mo—O distance(s) (Å) | $\Sigma S_i$ | $V - \Sigma S_i$ | Hydrogen-bond acceptor function |
|---|---|---|---|---|---|
| O1 | Terminal | 1.717 (2) | 1.671 | −0.329 | N—H···O |
| O3 | Terminal | 1.709 (2) | 1.708 | −0.292 | O—H···O |
| O6 | Terminal | 1.704 (2) | 1.731 | −0.269 | N—H···O |
| O8 | Terminal | 1.693 (2) | 1.783 | −0.217 | N—H···O |
| O11 | Terminal | 1.702 (2) | 1.740 | −0.260 | None |
| O13 | Terminal | 1.701 (2) | 1.745 | −0.255 | N—H···O |
| O2 | $\mu_2$ | 1.917 (2), 1.977 (2) | 1.801 | −0.199 | N—H···O |
| O4 | $\mu_2$ | 1.901 (2), 1.960 (2) | 1.883 | −0.117 | O—H···O |
| O9 | $\mu_2$ | 1.755 (2), 2.276 (2) | 1.877 | −0.123 | None |
| O12 | $\mu_2$ | 1.767 (2), 2.137 (2) | 1.997 | −0.003 | None |
| O7 | $\mu_3$ | 1.920 (2)–2.173 (2) | 2.028 | 0.028 | None |
| O10 | $\mu_3$ | 1.914 (2)–2.317 (2) | 1.733 | −0.267 | N—H···O |
| O5 | $\mu_4$ | 1.930 (2)–2.438 (2) | 1.952 | −0.048 | |

## Compound (II)

*Crystal data*

$(C_{10}H_{16}N_4)_2[SiMo_{12}O_{40}]\cdot 4H_2O$
$M_r = 2275.97$
Monoclinic, $C2$
$a = 22.5418$ (14) Å
$b = 20.4965$ (10) Å
$c = 12.5203$ (8) Å
$\beta = 110.270$ (8)°
$V = 5426.5$ (6) Å$^3$
$Z = 4$
Mo $K\alpha$ radiation
$\mu = 2.81$ mm$^{-1}$
$T = 173$ K
0.16 × 0.12 × 0.10 mm

*Data collection*

Stoe IPDS diffractometer
Absorption correction: numerical [*X-RED* (Stoe & Cie, 2001) and *X-SHAPE* (Stoe & Cie, 1999)]
$T_{min} = 0.662$, $T_{max} = 0.766$
23905 measured reflections
12670 independent reflections
11002 reflections with $I > 2\sigma(I)$
$R_{int} = 0.028$

*Refinement*

$R[F^2 > 2\sigma(F^2)] = 0.027$
$wR(F^2) = 0.056$
$S = 0.91$
12670 reflections
775 parameters
1 restraint
H-atom parameters constrained
$\Delta\rho_{max} = 1.59$ e Å$^{-3}$
$\Delta\rho_{min} = -1.45$ e Å$^{-3}$
Absolute structure: Flack (1983), with 5860 Friedel pairs
Flack parameter: 0.29 (2)

**Table 3**
Hydrogen-bond geometry (Å, °) for (II).

| $D$—H···$A$ | $D$—H | H···$A$ | $D$···$A$ | $D$—H···$A$ |
|---|---|---|---|---|
| O1$W$—H1$W$···O32$^{i}$ | 0.85 | 2.15 | 2.974 (5) | 164 |
| O1$W$—H2$W$···O8$^{ii}$ | 0.85 | 2.02 | 2.814 (6) | 156 |
| O2$W$—H3$W$···O26$^{iii}$ | 0.85 | 2.21 | 3.048 (6) | 171 |
| O2$W$—H4$W$···O4$W^{iv}$ | 0.85 | 2.31 | 3.012 (6) | 139 |
| O3$W$—H5$W$···O12$^{v}$ | 0.85 | 1.98 | 2.802 (6) | 163 |
| O3$W$—H6$W$···O20$^{iii}$ | 0.85 | 2.33 | 2.991 (5) | 134 |
| O3$W$—H6$W$···O25$^{iii}$ | 0.85 | 2.43 | 3.151 (6) | 143 |
| O4$W$—H7$W$···O36$^{i}$ | 0.85 | 2.12 | 2.910 (6) | 154 |
| O4$W$—H7$W$···O28$^{i}$ | 0.85 | 2.58 | 3.206 (6) | 131 |
| O4$W$—H8$W$···O22$^{vi}$ | 0.85 | 2.59 | 3.076 (7) | 117 |
| O4$W$—H8$W$···O2$W^{vii}$ | 0.85 | 2.64 | 3.012 (6) | 108 |
| N1—H1···O8 | 0.88 | 2.17 | 2.999 (6) | 156 |
| N2—H2···O4$W$ | 0.88 | 2.03 | 2.864 (7) | 157 |
| N3—H3···O1 | 0.88 | 2.23 | 2.966 (6) | 141 |
| N3—H3···O18 | 0.88 | 2.50 | 3.285 (6) | 148 |
| N4—H4···O1$W$ | 0.88 | 1.82 | 2.693 (6) | 172 |
| N5—H5···O3$W$ | 0.88 | 2.15 | 2.776 (6) | 128 |
| N5—H5···O19$^{iii}$ | 0.88 | 2.55 | 3.041 (6) | 116 |
| N6—H6···O4 | 0.88 | 2.07 | 2.866 (6) | 150 |
| N7—H7···O2$W$ | 0.88 | 1.93 | 2.789 (7) | 165 |
| N8—H8···O12 | 0.88 | 2.10 | 2.896 (6) | 150 |
| N8—H8···O1$^{viii}$ | 0.88 | 2.58 | 3.107 (6) | 120 |

Symmetry codes: (i) $-x+\frac{1}{2}, y-\frac{1}{2}, -z+2$; (ii) $x, y, z+1$; (iii) $-x+\frac{1}{2}, y+\frac{1}{2}, -z+1$; (iv) $x, y+1, z$; (v) $x, y, z-1$; (vi) $-x+\frac{1}{2}, y-\frac{1}{2}, -z+1$; (vii) $x, y-1, z$; (viii) $-x+\frac{1}{2}, y+\frac{1}{2}, -z+2$.

**Table 4**
Bond-valence sums for $[SiMo_{12}O_{40}]^{4-}$ anions and hydrogen-bond functionality of the oxide ligands in (II).

The details are as given in Table 2. The bond-valence sums for the Mo atoms are $\Sigma S_i$ = 5.877–5.970.

| O-atom type | Mo—O bond range (Å) | $\Sigma S_i$ range | $V - \Sigma S_i$ mean | No. of O atoms | O—H···O | N—H···O |
|---|---|---|---|---|---|---|
| Terminal | 1.677 (4)–1.711 (4) | 1.698–1.862 | −0.211 | 12 | 2 | 5 |
| $\mu_2$ | 1.824 (4)–2.043 (4) | 1.771–2.019 | −0.083 | 24 | 7 | 2 |
| $\mu_4$ | 2.311 (3)–2.385 (3) | 1.905–1.943 | −0.076 | 4 | | |

All methyl H atoms were added geometrically, while N- and O-bound H atoms were located from difference maps and then geometrically optimized and refined as riding on their parent atom. O—H distances were constrained to 0.85 Å, N—H distances to 0.88 Å and C—H distances to 0.98 Å, with $U_{iso}$(H) = 1.5$U_{eq}$(C,N,O).

For both compounds, data collection: *IPDS Software* (Stoe & Cie, 2000); cell refinement: *IPDS Software*; data reduction: *IPDS Software*; program(s) used to solve structure: *SHELXS97* (Sheldrick, 2008); program(s) used to refine structure: *SHELXL97* (Sheldrick, 2008); molecular graphics: *DIAMOND* (Brandenburg, 1999); software used to prepare material for publication: *WinGX* (Farrugia, 1999).

The authors acknowledge support from the Deutsche Forschungsgemeinschaft (grant No. UKR 17/1/06) and from the State Fund for Fundamental Research of Ukraine (DFFD) (grant No. 09DF037-03).

Supplementary data for this paper are available from the IUCr electronic archives (Reference: KU3054). Services for accessing these data are described at the back of the journal.

## References


Boldog, I., Daran, J.-C., Chernega, A. N., Rusanov, E. B., Krautscheid, H. & Domasevitch, K. V. (2009). *Cryst. Growth Des.* **9**, 2895–2905.
Boldog, I., Rusanov, E. B., Chernega, A. N., Sieler, J. & Domasevitch, K. V. (2001). *Angew. Chem. Int. Ed.* **40**, 3435–3440.
Boldog, I., Rusanov, E. B., Sieler, J. & Domasevitch, K. V. (2004). *New J. Chem.* **28**, 756–759.
Brandenburg, K. (1999). *DIAMOND*. Release 2.1e. Crystal Impact GbR, Bonn, Germany.
Dang, D.-B. & Jin, Y.-N. (2007). *Acta Cryst.* E**63**, m881–m883.
Domasevitch, K. V. (2008). *Acta Cryst.* C**64**, o326–o329.
Fang, R.-Q., Zhang, X.-M., Wu, H.-S. & Ng, S. W. (2004). *Acta Cryst.* E**60**, m359–m361.
Farrugia, L. J. (1999). *J. Appl. Cryst.* **32**, 837–838.
Flack, H. D. (1983). *Acta Cryst.* A**39**, 876–881.
Hagrman, P. J., Hagrman, D. & Zubieta, J. (1999). *Angew. Chem. Int. Ed.* **38**, 2638–2684.
Halcrow, M. A. (2009). *Dalton Trans.* pp. 2059–2073.
Hubbard, D. J., Johnston, A. R., Casalongue, H. S., Narducci Sarjeant, A. & Norquist, A. J. (2008). *Inorg. Chem.* **47**, 8518–8525.
Liu, H., Su, L., Wang, L. & Li, W. (2010). *Acta Cryst.* E**66**, m443–m444.
Nelson, J. R., Narducci Sarjeant, A. & Norquist, A. J. (2006). *Acta Cryst.* E**62**, m1731–m1733.
Rusanov, E. B., Ponomarova, V. V., Komarchuk, V. V., Stoeckli-Evans, H., Fernandez-Ibanez, E., Stoeckli, F., Sieler, J. & Domasevitch, K. V. (2003). *Angew. Chem. Int. Ed.* **42**, 2499–2501.
Sheldrick, G. M. (2008). *Acta Cryst.* A**64**, 112–122.
Singh, U. P., Kashyap, S., Singh, H. J. & Butcher, R. J. (2011). *CrystEngComm*, **13**, 4110–4120.
Stoe & Cie (1999). *X-SHAPE*. Revision 1.06. Stoe & Cie GmbH, Darmstadt, Germany.
Stoe & Cie (2000). *IPDS Software*. Stoe & Cie GmbH, Darmstadt, Germany.
Stoe & Cie (2001). *X-RED*. Version 1.22. Stoe & Cie GmbH, Darmstadt, Germany.
Thorn, K. J., Narducci Sarjeant, A. & Norquist, A. J. (2005). *Acta Cryst.* E**61**, m1665–m1667.
Tytko, K. H., Mehmke, J. & Fischer, S. (1999). *Struct. Bond.* **93**, 129–321.
Xu, Y., An, L.-H. & Koh, L.-L. (1996). *Chem. Mater.* **8**, 814–818.
Yu, S.-Y., Huang, H.-P., Li, S.-H., Jiao, Q., Li, Y.-Z., Wu, B., Sei, Y., Yamaguchi, K., Pan, Y.-J. & Ma, H.-W. (2005). *Inorg. Chem.* **44**, 9471–9488.
Zhang, J.-P. & Kitagawa, S. (2008). *J. Am. Chem. Soc.* **130**, 907–917.